IEEE Access
Multidisciplinary | Rapid Review | Open Access Journal

Received 3 December 2022, accepted 19 December 2022, date of publication 29 December 2022, date of current version 5 January 2023.

Digital Object Identifier 10.1109/ACCESS.2022.3233103

RESEARCH ARTICLE

Waveform Design and DoA-DoD Estimation of OFDM-LFM Signal Based on SDFnT for MIMO Radar

JINGQI WANG, (Member, IEEE), PINGPING WANG, FAN LUO, AND WEN WU, (Senior Member, IEEE)
Ministerial Key Laboratory of JGMT, Nanjing University of Science and Technology, Nanjing 210094, China
Corresponding author: Jingqi Wang (wangjingqi@njust.edu.cn)

ABSTRACT In comparison to orthogonal frequency division multiplexing (OFDM), the OFDM linear frequency modulation (OFDM-LFM) signal has similar time-bandwidth product, lower peak-to-average power ratio, and higher sensitivity to Doppler frequency shift, making it a promising candidate waveform for multiple-in multiple-out (MIMO) radar applications. However, the OFDM-LFM signal is unsatisfactory in practical applications due to the challenges in waveform design and its non-stationary property, which significantly degrades the performance of current high-resolution subspace techniques for direction of departure (DoD) and direction of arrival (DoA) angle estimation. In this paper, we first proposed a novel OFDM-LFM waveform design method based on the scale discrete Fresnel transform (SDFnT), which efficiently generates orthogonal LFM signals with unlimited number of subcarriers and can be convieniently implemented using the fast Fourier transform (FFT). Then, for angle estimation in OFDM-LFM MIMO radars, we presented a new scale discrete Fresnel transform multiple signal classification (SDFnT-MUSIC) method. By converting the steering vector into the chirp domain and making it non-time-vary, high resolution angle estimation for OFDM-LFM wideband signals can be achieved. Simulation results shows that the proposed waveform design method requires less computational time than conventional method based based on the fractional Fourier transform (FrFT), whereas the proposed DoA-DoD estimation method outperform the FrFT-MUSIC method in terms of computational complexity and target angle estimate performance.

INDEX TERMS MIMO radar, MUSIC, DoA, DoD, SDFnT, OFDM-LFM.

I. INTRODUCTION

In recent years, multiple-input multiple-output (MIMO) radar systems have been prosperously developed due to their high power efficiency, great flexibility, powerful anti-interference capability, and effective weak target detection [1], [2], [3], [4], [5], [6]. Orthogonal frequency division multiplexing (OFDM) signal, which is commonly used in communication systems, has become a widely accepted waveform for MIMO radars because of its subcarriers' mutual orthogonality broad bandwidth, high range resolution, adaptability and ease of generation of transmit signals [7], [8], [9], [10]. As a combination of OFDM and linear frequency modulation (LFM) signals, the OFDM-LFM signal consists of a group of mutually orthogonal LFM signals in each subcarrier that can be directly fed into different antennas of the MIMO radar system, and therefore provides the same benefits for MIMO applications as OFDM signals. Furthermore, the OFDM-LFM signal outperforms OFDM signals in terms of peak-to-average power ratio (PAPR) and Doppler tolerance [11], [12], making it a promising candidate waveform for MIMO radar.

The primary challenge in waveform design for OFDM-LFM based MIMO radar is how to efficiently generate numerous orthogonal LFM signals. J. H. Kim suggested to produce OFDM-LFM signals by inserting extra zeros between the subcarriers [13], [14], which leads to a drastically increase in pulse duration as the number of subcarriers

The associate editor coordinating the review of this manuscript and approving it for publication was Guolong Cui.

grows. S. J. Cheng enhanced the number of OFDM-LFM subcarriers [15] by combining the OFDM LFM scheme and direct sequence spread spectrum approach, but the quantity of generated orthogonal waveforms remains insufficient. Y. Q. Wang proposed utilizing a random matrix to modulate OFDM-LFM waveforms [16] which can produce more than three orthogonal waveforms simultaneously but suffers from high sidelobes of the ambiguity function and complicated waveform production. A technique for generating an OFDM-LFM orthogonal waveform using the fractional Fourier transform (FrFT) method is described in the literatures [17], [18], [19]. This approach has the advantage of producing any desired number of subcarriers at the same time while satisfying orthogonality and having good correlation characteristics, but it has the disadvantage of being computationally complex.

Another major current focus in OFDM-LFM based MIMO radar research is the high resolution angle estimation with LFM non-stationary signal. MIMO radars can virtually extend the antenna array and enlarge the aperture, allowing it to achieve precise angle estimation that requires extensive spatial sampling. High resolution angle estimation methods for OFDM-based MIMO radars have generated considerable recent research interest [20], [21], [22], [23]. Unfortunately, when applied to OFDM-LFM-based MIMO radars, the performance of these traditional approaches degrades significantly. This is due to the fact that the subcarrier frequency of OFDM-LFM waveform changes with time rather than being constant, and the steering vector of the OFDM-LFM-based MIMO radar varies with not only the incident angle but also the time. Time-frequency (TF) analysis methods, including wavelet transform (WT), Wigner-Ville Distribution (WVD) method, short-time Fourier transform (STFT) and FrFT, etc, can explore the joint time-frequency properties of non-stationary signals by transforming the signals to the time-frequency domain [24], [25], [26], [27], and can thus be combined with traditional array signal processing methods to achieve high resolution angle estimation with LFM-like non-stationary signals. Hurstman et al. proposed a time-frequency coherent signal subspace technique based on the WVD for LFM-like nonstationary signals [28], whereas the cross-term interference severely degrades the performance of direction of arrival (DoA) estimate for multiple targets. While the STFT can avoid the cross-term interference, improper window selection can readily result in a reduction in estimation accuracy. Due to its flexible time-frequency focusing property for non-stationary signals and high robustness against cross-term interference, FrFT was used for DoA estimation of multi-component LFM signals in [30], however, it still suffers from its computational cost.

In this paper, we first propose an efficient OFDM-LFM waveform design method based on a novel scale discrete Fresnel transform (SDFnT), whose kernel function is a set of orthogonal LFM with adjustable chirp rate. In order to achieve high-precision estimation of transceiver angle for MIMO radars using non-stationary signals, we further propose a novel DoA-DoD (direction of departure) estimation method for OFDM-LFM-based MIMO system by combining the SDFnT method with the high-resolution multiple signal classification algorithm (MUSIC) algorithm. Since the proposed SDFnT is discrete Fourier transform (DFT) compatible, the proposed SDFnT-based waveform design and angle estimation methods have lower computational complexity than FrFT-based methods and can be efficiently implemented in the existing OFDM MIMO systems. The main contributions of this article are summarized below.

1) A fast OFDM-LFM waveform design method is proposed for MIMO radar applications. It is derived from the SDFnT, a deformation of the Fresnel transform, and can be easily implemented by multipying the scaled phase matrice and the fast Fourier transform. The effectiveness of the generated signals is validated by ultilizing ambiguity function.
2) A novel angle estimation for OFDM-LFM wideband signals is presented. The SDFnT-based method compensates the time-varying steering vector and converts it to a non-time-varying steering vector. The MUSIC method is combined further to achieve high resolution angle estimation.
3) A DoA-DoD estimation for bistatic OFDM-LFM-based MIMO radar is porposed based on the aforementioned method.
4) The Cramer-Rao Bound (CRB) of angle estimation of broadband signal under the uniform linear array (ULA) model is derived.
5) Numerical simulations are provided to evaluate the superiority of the proposed methods in terms of estimation accuracy and computational complexity compared with previous ones.

The division of this article is as follows. Section II of this article covers the design of the OFDM-LFM-based MIMO orthogonal waveform, along with its computational complexity and ambiguity function analysis.Section III discusses about the invalidation of the conventional MUSIC algorithm of non-stationary OFDM-LFM signals, and proposes a novel high-resolution angle estimation method by combining the SDFnT method with the MUSIC algorithm. Section IV gives the simulation results. Finally, section V outlines the conclusion of the study.

Throughout this article, the boldface italic letters are used to represent vectors, matrices, and tensors. The Kronecker product of $\boldsymbol{A}$ and $\boldsymbol{B}$ is set as $\boldsymbol{A} \otimes \boldsymbol{B}$. The notation diag $(\cdot)$ represhents a diagonal matrix. $\boldsymbol{I}_L$ is a $L \times L$ identity matrix, $\mathrm{E}[\cdot]$ denotes the expectation operator. mod means take the remainder, $(\cdot)^*$ means conjugation, $(\cdot)^T$ stands for transpose, tr$(\cdot)$ represents the trace of the matrix.

II. MIMO ORTHOGONAL WAVEFORM DESIGN

In this section, an efficient OFDM-LFM waveform design method is presented. Firstly, a scale discrete Fresnel transform developed from the discrete Fresnel transform (DFnT),

an integral transformation comes from classical optics [33], [34], [35], [36], is proposed, and then a novel OFDM-LFM waveform design method based on it is presented for MIMO radar.

A. SDFnT-BASED OFDM-LFM WAVEFORM DESIGN

The kernel functions of the proposed SDFnT are a set of orthogonal chirp signals. Unlike the conventional DFnT with fixed chirp rate, the chirp rate of the SDFnT kernel fucntion is adjustable and controlled by a non-zero scale transform factor. By varying the scale transformation factor, more types of orthogonal waveforms as well as improved interception resistance and radar detection performance can be developed.The n-th chirp signal of the proposed OFDM-LFM waveform is defined as

$$\psi_n(t) = e^{j\frac{\pi}{4}} e^{-j\pi \frac{N}{T^2}\left(t\cdot\alpha - n\frac{T}{N\alpha}\right)^2} \tag{1}$$

where T is the duration of the chirp basis signal, N is the number of chirps, namely the number of subcarriers, and α is the scale transformation factor.

The discrete expression of OFDM-LFM is as follows:

$$s(n) = \frac{1}{\sqrt{N}} e^{j\frac{\pi}{4}} \sum_{k=0}^{N-1} x(k) \times \begin{cases} e^{-j\frac{\pi}{N}\left(\frac{m}{\alpha} - n\alpha\right)^2} & N \equiv 0\,(mod 2) \\ e^{-j\frac{\pi}{N}\left(\frac{m}{\alpha} - n\alpha + \frac{1}{2}\right)^2} & N \equiv 1\,(mod 2) \end{cases} \tag{2}$$

in this equation, m and n stand for the numbers of sample points in the time and frequency domains, As can be easily seen from the aforementioned equation, the time-frequency characteristics of this OFDM-LFM signal consist of a collection of diagonal lines that are mutually parallel and have a controlled chirp rate. Let the bandwidth of th signal be B, then the chirp spacing is $\Delta f = B/N$, the initial frequency and tuning slope of the n-th chirp is $f_0 = n\Delta f$ and $B/\alpha^2 T$ respectively. This collection of chirp signals has varied initial frequencies that are proportional to the number of subcarriers, but they all have the same tuning slope. It behaves as a series of mutually parallel diagonal lines in the time-frequency plane, similar to LFM signals with step-frequency, thus increasing spectrum efficiency. The chirp rate of this collection of chirp signals varies with the transformation factor α.

As shown by the following, the chirp signals in equation 1 are mutually orthogonal,

$$\begin{aligned} &\int \psi_p^*(t)\psi_q(t)dt \\ &= \int_0^T e^{j\pi\frac{N}{T^2}\left(\frac{t}{\alpha} - \frac{pT}{N}\alpha\right)^2} e^{-j\pi\frac{N}{T^2}\left(\frac{t}{\alpha} - \frac{pT}{N}\alpha\right)^2} dt \\ &= \begin{cases} Te^{j\frac{\pi}{N}(\rho^2 - q^2)\alpha^2} & p = q \\ 0 & p \neq q \end{cases} \end{aligned} \tag{3}$$

where p and q represent the p-th sub-carrier and the q-th sub-carrier, respectively.

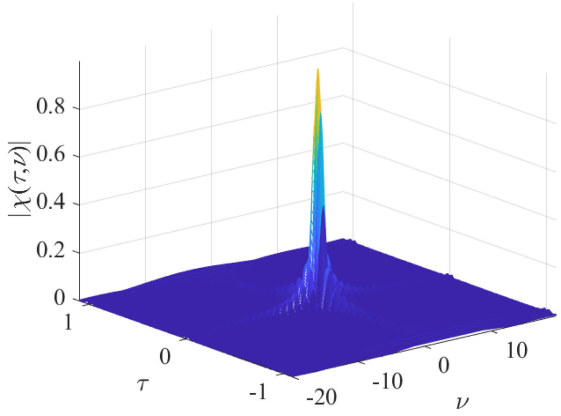

FIGURE 1. $\alpha = 0.25j$, 3D ambiguity fuction of OFDM-LFM.

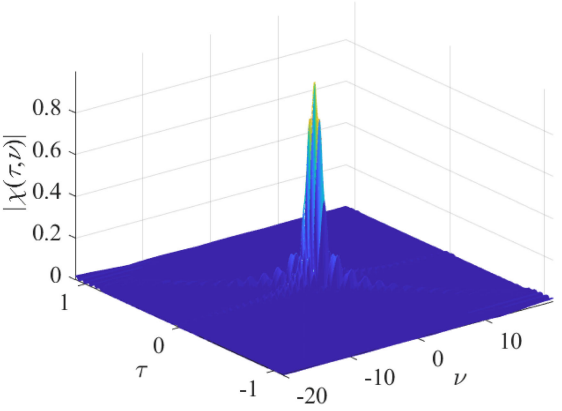

FIGURE 2. $\alpha = 4j$, 3D ambiguity fuction of OFDM-LFM.

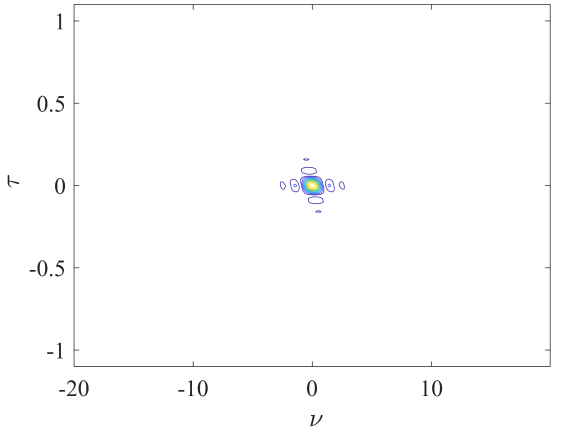

FIGURE 3. $\alpha = 0.25j$, top view of OFDM-LFM ambiguity fuction.

We define the (m, n)th element of the N by N SDFnT matrix as

$$\mathbf{\Phi}_\alpha(m,n) = \frac{e^{-j\frac{\pi}{4}}}{\sqrt{N}} \times \begin{cases} e^{j\frac{\pi}{N}\left(\frac{m}{\alpha} - n\alpha\right)^2} & N \equiv 0\,(mod 2) \\ e^{j\frac{\pi}{N}\left(\frac{m}{\alpha} + \frac{1}{2} - n\alpha\right)^2} & N \equiv 1\,(mod 2) \end{cases} \tag{4}$$

In order to comply with the practical OFDM system, N is set to be an even number, and we can thus simplify the

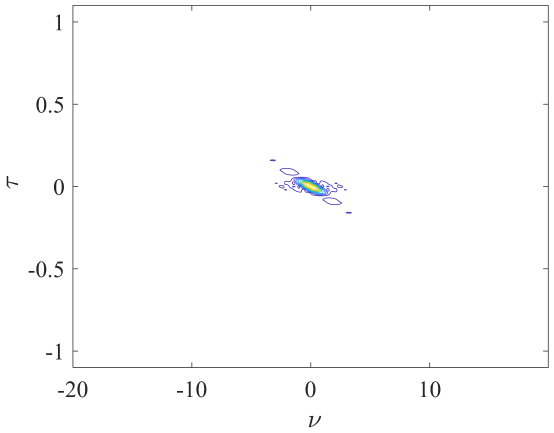

FIGURE 4. $\alpha = 4j$, **top view of OFDM-LFM ambiguity fuction.**

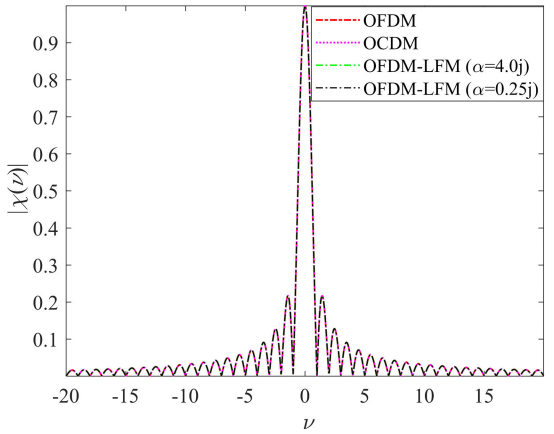

FIGURE 5. Comparison of velocity ambiguity fuctions of different orthogonal waveforms.

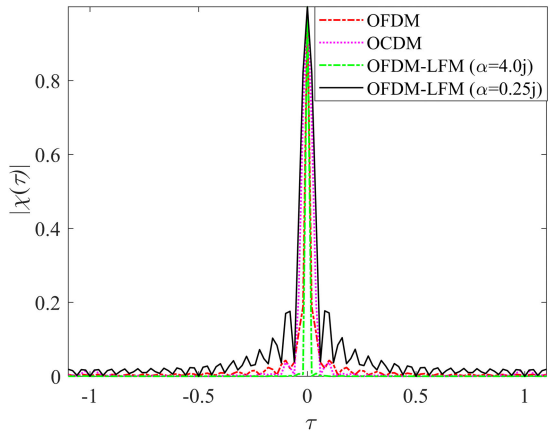

FIGURE 6. Comparison of range ambiguity fuctions of different orthogonal waveforms.

definition of SDFnT matrix $\mathbf{\Phi}_\alpha \in C N \times N$ as

$$\mathbf{\Phi}_\alpha(m,n) = \frac{1}{\sqrt{N}} e^{-j\frac{\pi}{4}} \times e^{j\frac{\pi}{N}\left(\frac{m}{\alpha}\right)^2} e^{-j\frac{2\pi}{N}mn} e^{j\frac{\pi}{N}(n\alpha)^2} \tag{5}$$

The expression of the classical Fourier transform is

$$\boldsymbol{F}(m,n) = \frac{1}{\sqrt{N}} e^{-j\frac{2\pi}{N}mn} \tag{6}$$

$\boldsymbol{F}$ is the discrete Fourier transform matrix.

Clearly, $\mathbf{\Phi}_\alpha(m,n)$ can be represented in matrix form as

$$\mathbf{\Phi}_\alpha = \mathbf{\Theta}_1 \boldsymbol{F} \mathbf{\Theta}_2 \tag{7}$$

where

$$\mathbf{\Theta}_1 = \mathrm{diag}(\boldsymbol{\theta}_1(m)) \in C^{N\times N}, m = 0, 1, \ldots, N-1 \tag{8}$$

$$\mathbf{\Theta}_2 = \mathrm{diag}(\boldsymbol{\theta}_2(n)) \in C^{N\times N}, n = 0, 1, \ldots, N-1 \tag{9}$$

where $\boldsymbol{\theta}_1(m) = \mathrm{e}^{j\frac{\pi}{4}} \mathrm{e}^{j\frac{\pi}{N}\left(\frac{m}{\alpha}\right)^2}, m = 1, 2, \cdots M-1, \boldsymbol{\theta}_2(n) = \mathrm{e}^{j\frac{\pi}{N}n\alpha^2}, n = 1, 2, \cdots N-1.$

Equation 7 makes it apparent that the SDFnT is DFT-compatible because it can be implemented using DFT and phase matrix multiplications. as the result,the OFDM-LFM waveform developed in this paper is compatible with current OFDM systems while having a lower peak-to-average ratio than the OFDM waveform, making the SDFnT-based waveform design method presented in this paper more practical in waveform synthesis than the method proposed in the literatures [17], [18], [19]. Additionally, because the SDFnT has an inverse transform, it is suitable for modulation and demodulation in communication systems, as well as joint radar and communication (JRC) systems.

B. ANALYSIS OF COMPUTATIONAL

In this subsection, we compare the computational complexity of the SDFnT and FrFT in terms of time complexity, which is the trend of code execution time as data size changes and typically represented by a large O representation. The execution time of algorithm is given as

$$T[n] = O(f(n)) \tag{10}$$

where $T[n]$ denotes the code execution time, n is the size of the data scale, and $f(n)$ denotes the total of the number of times each line of code is run.

As is well known, the N points discrete Fourier transform (DFT) algorithm requires N^2 complex multiplication operations and $N(N-1)$ complex additional operations, therefore the time complexity of the DFT algorithm is $O(N^2)$. In contrast, the fast Fourier transform (FFT) algorithm, an effective and practical DFT algorithm with the basic operation modules as the butterfly operation with radix-2, requires $\frac{N}{2} \times \log_2^N$ complex multiplication operations and $N \times \log_2^N$ complex addition operations, respectively [31]. As a result, the FFT algorithm's time complexity is reduced to $O(N \times \log_2^N)$. As described in Section II-A, the proposed SDFnT algorithm is DFT-compatible, then it can be effectively implemented by FFT operation and two additional phase rotations. For the length of N, the time complexity of FrFT algorithm is $T(N) = O(N^2)$ [32], whereas the time complexity of SDFnT is $T(N) = O(N \times \log_2^N)$. Evidently, SDFnT has a lower computational complexity than FrFT.

C. ANALYSIS OF RADAR AMBIGUITY FUCTION

One of the crucial performance indicators for radar waveform analysis is the ambiguity function (AF), which can accurately

assess the autocorrelation performance of radar signals, parametric traits, as well as Doppler shift and distance ambiguity. The performance analysis of the proposed OFDM-LFM signal is provided in this part from the viewpoint of the radar ambiguity fuction.

Figure 1 and Figure 3 show the ambiguity function of the SDFnT-based OFDM-LFM signal with the scale transformation factor value of 0.25j in 3D view and in top view respectively, while Figure 2 and Figure 4 demostrate the AF with the value of 4j. These four figures can be compared to show that as the value of the scale transformation factor increases, the modulation slope of OFDM-LFM declines, the velocity resolution of the OFDM-LFM radar remains constant, and the range resolution decreases.

Figure 5 compares the zero Doppler cuts of the ambiguity functions of OFDM, OCDM [33], and the proposed OFDM-LFM signal with different scale transformation factors, while Figure 6 compares the zero time delay cuts. Here, the OCDM is analyzed as a special example of the proposed SDFnT-based OFDM-LFM signal with the value of scale transformation factor set to 1. The velocity ambiguity functions of the four signals are nearly identical, as shown in Figure 5, indicating that they have similar velocity resolution. The range ambiguity function in Figure 6 reveals that the main lobe of an OFDM signal is narrower than that of an OCDM signal. Furthermore, when $|\alpha| < 1$, as in the curve corresponding to $\alpha = 0.25$j, the main lobe of the proposed signal is wider than OCDM and the side lobe is higher; when $|\alpha| > 1$, as in the curve corresponding to $\alpha = 4$j, the main lobe becomes the narrowest and the side lobe becomes the lowest of the four simulated signals.

III. ANGLE ESTIMATION BASED ON SDFnT

This section's major topic is the bistatic MIMO radar multi-target estimatin problem for the DoD and DoA. A detailed description of the conventional MUSIC algorithm, a high-resolution DoA estimation approach [37], as well as the issues that can arise when using the MUSIC algorithm to estimate DoA for non-stationary signals is presented. We first convert the received wideband OFDM-LFM signals from the time domain into the chirp domain by using the SDFnT algorithm. Next, we establish the steering vector in the chirp domain, which won't change with the frequency and will have the same characteristics as the steering vector of the narrowband signal if the appropriate scale factor is applied. As a result, the conventional high resolution algorithm can be used to estimate the transmitting and receiving angles for non-stationary OFDM-LFM signals.

A. MIMO RADAR SYSTEM MODEL

The bistatic MIMO radar model is depicted in Figure 7. Each transmitting array element transmits a single OFDM-LFM subcarrier, and each subcarrier, which resembles a series of frequency-stepped LFM signals, has a distinct beginning frequency and the same tuning slope. We can synthesize a virtual uniform linear array of $Mt * Mr$ using bistatic MIMO

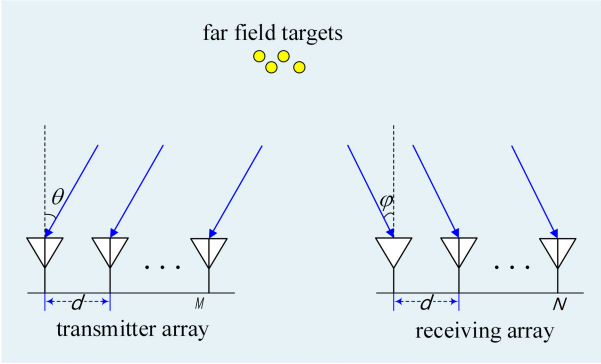

FIGURE 7. Bistatic MIMO radar model.

radar with Mt transmitting antenna and Mr receiving antenna. The array model satisfies the following conditions:

(1) the sources meet the requirement for a far-field, they are uncorrelated with one another, and more virtual array members are present than desired;
(2) the receiving array is an ULA with a less than half-wavelength array spacing;
(3) zero-mean Gaussian white noise (AWGN) makes up the noise signal;

The array signal's received data model can be obtained as

$$\boldsymbol{X}(t) = \boldsymbol{A}\boldsymbol{S}(t) + \boldsymbol{N}(t) \tag{11}$$

where $\boldsymbol{A} = [a(\theta_1), a(\theta_2), \cdots, a(\theta_K)]^T$ is $M \times K$ dimension steering vector, $s(t)$ if $K \times 1$ dimension vector of wideband nonstationary source waveforms, $\boldsymbol{N}(t)$ is $M \times 1$ dimension vector of zero-mean Gaussian white noise. M is the number of receiving virtual array elements, while K is the number of snapshots. θ_K is the incident angle of the K-th signal. $a(\theta_k) = \left[1, e^{-j\varphi_{2k}}, \cdots, e^{-j\varphi_{Mk}}\right]^T$, $k = 1, 2, \cdots, K$ is the steering vector for the k-th signal. Under the condition of narrowband stationary, the phase term $\varphi_{mk} = 2\pi(m-1)d\sin\theta_k/\lambda$ in the steering vector is only related to the angle θ_k, and is independent of time t, λ stands for wavelength and d is the receiving array element spacing.

The core process in the MUSIC algorithm is to build the signal's covariance matrix and perform eigen decomposition. The eigen vector is then split into signal and noise subspaces. Finally, the MUSIC spectrum is built and the high resolution DoA estimation is achieved by spectral peak searching. However, the classic MUSIC algorithm only works with narrowband signals and is ineffective with non-stationary signals like OFDM-LFM signals.

Assuming that there are k non-stationary signals incident on the above uniform linear array in the far field, the output signal of the m-th array element is

$$x^m(t) = \sum_{k=1}^{K} s_k(t - \tau_k^m) + n^m(t) \tag{12}$$

where $s_k(t) = e^{j2\pi\left(k\cdot\Delta f\cdot t + \frac{1}{2}\mu_k t^2\right)}$ is the k-th incident non-stationary signal, $f_k = k\cdot\Delta f$ is the initial frequency of the k-th

subcarrier of OFDM-LFM signal and Δf is the frequency separation between the two signals, μ_k is the frequency modulation slope, $n^m(t)$ is the noise signal of the m-th element. Substituting the above equation into $\boldsymbol{X}(t) = \boldsymbol{A}\boldsymbol{S}(t) + \boldsymbol{N}(t)$ and simplifying, the time-varying direction vector of the k-th incident signal on M receiving elements can be obtained as follows:

$$a_k(t) = \left[1, e^{-j2\pi f_k t \tau_k^1} e^{j\pi\mu_k(\tau_k^1)^2}, \cdots, e^{-j2\pi f_k t \tau_k^M} e^{j\pi\mu_k(\tau_k^M)^2}\right] \tag{13}$$

where $\tau_k^m = (m-1)\, d \sin\theta_k / c$ is the delay of the k-th signal on the m-th receiving array element, c is the speed in the medium where the received signal is located. It is evident from (13) that this direction vector is related to both time and the angle of the incident signal; hence, the classic DoA estimation method cannot be used.

B. SIGNAL MODEL

In this subsection, we proposed a novel SDFnT-based DoA estimation method for OFDM-LFM signal. The chirp domain signal after SDFnT transformation can be expressed as

$$\begin{aligned} \boldsymbol{X}_\alpha(n) &= \sum_{n=0}^{N-1} x(n) e^{j\frac{\pi}{4}} e^{-j\frac{\pi}{N}\left(\frac{m}{\alpha}-n\alpha\right)^2} \\ &= A e^{j\frac{\pi}{4}} e^{j\varphi} e^{-j\frac{\pi m^2}{N\alpha^2}} \sum_{n=0}^{N-1} e^{j\pi n^2\left(\mu-\frac{\alpha^2}{N}\right)} e^{j2\pi n\left(f_0+\frac{m}{N}\right)} \end{aligned} \tag{14}$$

The frequency modulation slope of the n-th subcarrier is $\mu = B/\alpha^2 T$, the bandwidth is B, and the center frequency is $f_0 = n\Delta f$. Firstly, the k-th LFM signal $s_k^1(t)$ received on the reference array element (zero delay) is discretized and SDFnT is performed to obtain the projection on the chirp domain $S_k^1(\alpha, u)$. Once the scale transformation factor α approaches the proper value, an energy-concentrated peak would appear in the chirp domain. The relationship between the scale transformation factor α and the frequency modulation slope μ is

$$\alpha = \alpha_k^1 = \sqrt{-\frac{1}{\mu \cdot L \cdot tb^2}} \tag{15}$$

where L is the number of fast sampling points in the time domain, tb is the sampling interval, and the spectral peak position is

$$u = u_k^1 = f_k \cdot L \cdot tb \tag{16}$$

The k-th incident signal received on the m-th element (when non-reference element delay is not zero) is

$$s_k^m(t) = s_k\left(t - \tau_k^m\right) = B_k\left(\tau_k^m\right) e^{j\pi\left[2(f_k-\mu_k\tau_k^m)t+\mu_k t^2\right]} \tag{17}$$

where $B_k\left(\tau_k^m\right) = e^{j\pi\left[\mu_k(\tau_k^m)^2 - 2f_k\tau_k^m\right]}$ is a constant term related only to delay and incident angle. Similarly, SDFnT transform is performed on $s_k^m(t)$ to obtain the rotation angle α and the spectral peak position u of $S_k^m(\alpha, u)$, as shown in (18) and (19), respectively:

$$\alpha = \alpha_k^m = \sqrt{-\frac{1}{\mu \cdot tb^2 \cdot L}} \tag{18}$$

$$u = u_k^m = \left(f_k - \mu\tau_k^m\right) \cdot L \cdot tb \tag{19}$$

As illustrated in (15) and (18), the scale transform factor is fixed while the spectral peak location changes for each array. By substituting (16) into (19) and simplifying it as follows, one can determine the relationship between the spectral peak location of the m-th receiving array element and that of the reference array element:

$$u_k^m = u_k^1 + \frac{\tau_k^m}{\alpha \cdot tb} \tag{20}$$

Then, compare the chirp domain projections of the reference array element and the m-th array element:

$$\boldsymbol{S}_k^1\left(\alpha_k, u_k^1\right) = e^{-j\frac{\pi}{4}} e^{j\frac{\pi}{L}\frac{\left(u_k^1\right)^2}{\alpha^2}} T \tag{21}$$

$$\boldsymbol{S}_k^m\left(\alpha_k, u_k^m\right) = e^{-j\frac{\pi}{4}} \boldsymbol{B}_k\left(\tau_k^m\right) e^{j\frac{\pi}{L}\frac{\left(u_k^m\right)^2}{\alpha^2}} T \tag{22}$$

Substituting (20) into (22), we get

$$\boldsymbol{S}_k^m\left(\alpha_k, u_k^m\right) = e^{-j\frac{\pi}{4}} \boldsymbol{B}_k\left(\tau_k^m\right) e^{j\frac{\pi}{L}\frac{\left(u_k^1+\frac{\tau_k^m}{\alpha\cdot tb}\right)^2}{\alpha^2}} T \tag{23}$$

Then, substituting (16) into the above formulas and simplifying it, we get

$$\begin{aligned} &\boldsymbol{S}_k^m\left(\alpha_k, u_k^m\right) \\ &= \boldsymbol{B}_k\left(\tau_k^m\right) e^{j2\pi f_k \frac{\tau_k^m}{\alpha}} e^{j\frac{\pi}{L}\frac{\left(\tau_k^m\right)^2}{(\alpha\cdot tb)^2}} e^{-j\frac{\pi}{4}} e^{j\frac{\pi}{L}\frac{\left(u_k^1\right)^2}{\alpha^2}} T \\ &= \boldsymbol{A}_k\left(\tau_k^m\right) \cdot \boldsymbol{S}_k^1\left(\alpha_k, u_k^1\right) \end{aligned} \tag{24}$$

Since $(\tau_k^m)^2 \ll 1$, the $e^{j\frac{\pi}{L}(\tau_k^m)^2/(\alpha\cdot tb)^2}$ term can be ignored. Finally, the expression of the direction vector of the k-th incident signal in the chirp domain after SDFnT is

$$\boldsymbol{A}_k = \left[1, A_k\left(\tau_k^2\right), \cdots, A_k\left(\tau_k^m\right)\right] \tag{25}$$

$$\boldsymbol{A}_k\left(\tau_k^m\right) = \boldsymbol{B}_k\left(\tau_k^m\right) e^{j2\pi f_k \frac{\tau_k^m}{\alpha}} \tag{26}$$

Regarding the angle of the k-th incident signal only, this vector is time-invariant under far-field conditions and exclusively related to the time-delay term τ_k^m. Instead of the conventional array signal model, this SDFnT-based signal model enables the transformation of the time-varying direction matrix of non-stationary signals that resemble OFDM-LFM into a fixed direction matrix, allowing DoA estimation by employing the conventional high-resolution methods.

Algorithm 1 DoA and DoD Estimation of OFDM-LFM Signal Based on SDFnT-MUSIC Method

Input: the signals $\mathbf{x}(t)$ received by the coprime array;

Output: the DoA and DoD estimation of the wideband signal $(\widehat{\theta}_k, \widehat{\varphi}_k)$;

1: Initialize: Perform SDFnT on the signal of the reference array element, then perform a spectral peak search (α_k, u) to get the number of incident signals;

2: SDFnT transform with a scaling factor of α_k for the received signals on all array elements in order to get the spectral peak location u_k^m and peak point data $\boldsymbol{X}_k^m\left(\alpha_k, u_k^m\right)$ of the k-th incident signal on the m-th array element;

3: $\boldsymbol{R}_k = \boldsymbol{X}_k \boldsymbol{X}_k^H$ the related matrix of the constructed chirp domain α

4: Perform eigenvalue decomposition on $\boldsymbol{R}_k$ to obtain the signal subspace matrix $\boldsymbol{U}_s$, and construct the spectral function $f\ (\theta, \varphi)$;

5: By traversing the transmitting angle θ and receiving angle φ and searching for the peaks of the spectrum $f\ (\theta, \varphi)$, find the incidence angle estimation of the K LFM signals.

C. ALGORITHM FLOW

The proposed SDFnT-based DoA and DoD estimation emthod for OFDM-LFM signal is briefllly summarized in Algorithm 1.

The proposed method, like the FrFT-based method, can estimate the number of targets but cannot identify multiple targets when they are very close.

D. ANALYSIS OF COMPUTATIONAL

We analyze the computational complexity of the proposed wideband signal angle estimation algorithm. For the propose 2D-MUSIC algorithm, time-frequency surface transformation requires $O\left\{PL\log_2^L\right\}$, calculating the covariance matrix needs $O\left\{L(MN)^2\right\}$, eigenvalue decomposition requires $O\left\{(MN)^3\right\}$, 2D angle finding costs $O\left\{\frac{90^\circ}{\Delta}\left[(MN+1)\left(MN-K\right)\right]\right\}$, so the proposed algorithm's overall computational complexity is $O\{PL\log_2^L + L(MN)^2 + (MN)^3 + \frac{90^\circ}{\Delta}\left[(MN+1)\left(MN-K\right)\right]\}$ where P is the number of time-frequency surface transformations, K is the number of targets, L is the number of snapshots, Δ is the angle search step value, N and M are the number of transmitting and receiving arrays, respectively.

E. CRB FOR WIDEBAND DoA ESTIMATION

The signal covariance matrix and noise covariance matrix for the received signal with unknown incident angle θ are, respectively

$$\boldsymbol{R}_s = \mathrm{E}\left[(\boldsymbol{a}\otimes\boldsymbol{s})(\boldsymbol{a}\otimes\boldsymbol{s})^H\right] = \sigma_s^2\boldsymbol{a}\boldsymbol{a}^H\otimes\boldsymbol{I}_L \tag{27}$$

$$\boldsymbol{R}_m = \mathrm{E}\left[\boldsymbol{n}\boldsymbol{n}^H\right] = \sigma_n^2\boldsymbol{I}_M\otimes\boldsymbol{I}_L = \boldsymbol{R}_1\otimes\boldsymbol{I}_L \tag{28}$$

among them, σ_s^2 and σ_n^2 are the signal power spectrum and noise power spectrum, respectively, $\boldsymbol{s}$ and $\boldsymbol{a}$ are signals and their steering vectors, $\boldsymbol{I}_L$ and $\boldsymbol{I}_M$ are the identity matrice, M is the number of receiving array elements, and L is the number of snapshots in the time domain. The received data covariance matrix is

$$\boldsymbol{R} = \boldsymbol{R}_s + \boldsymbol{R}_n = \left(\sigma_s^2\boldsymbol{a}\boldsymbol{a}^H + \boldsymbol{R}_1\right)\otimes\boldsymbol{I}_L. \tag{29}$$

The inverse matrix is

$$\begin{aligned}\boldsymbol{R}^{-1} &= \left(\boldsymbol{R}_1^{-1} - \frac{\boldsymbol{R}_1^{-1}\boldsymbol{a}\boldsymbol{a}^H\boldsymbol{R}_1^{-1}}{\sigma_s^{-2}+\boldsymbol{a}^H\boldsymbol{R}_1^{-1}\boldsymbol{a}}\right)\otimes\boldsymbol{I}_L \\ &= \left(\boldsymbol{R}_1^{-1} - \frac{\sigma_s^{-2}\boldsymbol{a}\boldsymbol{a}^H}{SNR^2 + M\cdot SNR^{-1}}\right)\otimes\boldsymbol{I}_L\end{aligned} \tag{30}$$

where the signal to noise ratio is $SNR \triangleq \sigma_s^2/\sigma_n^2$. According to [38], The likelihood function of the signal is

$$\boldsymbol{F}_1(\boldsymbol{r}) = \left(\pi^M\left|\boldsymbol{R}\right|\right)^{-1} e^{-\boldsymbol{r}^H\boldsymbol{R}^{-1}\boldsymbol{r}}. \tag{31}$$

For the unbiased estimator theta, its CRB is given by (32)

$$\mathrm{CRB} = \boldsymbol{J}^{-1} = \left\{-\mathrm{E}\left[\frac{\partial^2 ln\boldsymbol{F}_1(\boldsymbol{r})}{\partial\theta^2}\right]\right\}^{-1} \tag{32}$$

where the $\boldsymbol{J}$ matrix is called Fisher Information Matrix (FIM). Substituting (30) and (31) into Formula (32), we obtain

$$\begin{aligned}&\mathrm{CRB} \\ &= -\left\{L\frac{\partial^2}{\partial\theta^2}\mathrm{E}\left[\frac{\sigma_s^{-2}}{SNR^{-1}}\cdot\left(\boldsymbol{r}^H\boldsymbol{a}\boldsymbol{a}^H - \boldsymbol{r}^H\boldsymbol{R}_1^{-1}\boldsymbol{r}\right)\right]\right\}^{-1} \\ &= -\left\{\frac{L\sigma_s^{-2}}{SNR^{-2}+M\cdot SNR^{-1}}\cdot\mathrm{tr}\left[\frac{\partial^2}{\partial\theta^2}\left(\boldsymbol{a}\boldsymbol{a}^H\right)\mathrm{E}\left(\boldsymbol{r}\boldsymbol{r}^H\right)\right]\right\}\end{aligned} \tag{33}$$

In the case of only one incident angle, $\tau_{s,t} \triangleq \tau_s - \tau_t = \frac{\triangle_{s,t}}{c}$ is defined as the delay difference between the two array elements.

$$\boldsymbol{D}_{s,t} = \frac{\partial^2}{\partial\theta^2}e^{-j\omega\tau_{s,t}} = \left[-\frac{\omega^2\Gamma_{s,t}^2}{c^2} - j\frac{\omega\triangle_{s,t}}{c}\right]e^{-j\omega\tau_{s,t}} \tag{34}$$

among them $\Gamma_{s,t} = r_s cos(\theta+\varphi_s) - r_t cos(\theta+\varphi_t)$, then we get

$$\begin{aligned}\mathrm{tr}(\boldsymbol{F}) &= \sum_{s=0}^{M-1}\sum_{t=0}^{M-1}\sigma_s^2[-\frac{\omega^2\Gamma_{s,t}^2}{c^2} - j\frac{\omega\triangle_{s,t}}{c}] \\ &= \frac{\sigma_s^2\omega^2}{c^2}\sum_{s=0}^{M-1}\sum_{t=0}^{M-1}\Gamma_{s,t}^2.\end{aligned} \tag{35}$$

For the wideband signal, we divide it into $\boldsymbol{J}$ narrowband regions, and then the wideband CRB expression of far-field direction finding can be obtained as

$$\mathrm{CRB} = \frac{Mc^2}{4L\pi^2}(\sum_{s=0}^{M-1}\sum_{t=0}^{M-1}\Gamma_{s,t}^2)^{-1}\cdot P^{-1} \tag{36}$$

TABLE 1. computational time of FrFT and SDFnT.

methods	computational time (ms)			
	$N = 256$	$N = 768$	$N = 1280$	$N = 1792$
FrFT	15.84	130.26	394.65	892.69
SDFnT	12.66	104.65	303.92	661.85

$P = \sum_{i=0}^{J} \frac{Mf_i^2 \cdot SNR_i^2}{1+M \cdot SNR_i}$, f_i represents the center frequency of the i-th divided frequency band. SNR_i is the frequency domain signal to noise ratio on the i-th narrowband.

$$\mathrm{CRB} = \frac{3c^2}{2LM(M^2-1)\pi^2 d^2 cos^2\theta \cdot P} \tag{37}$$

IV. SIMULATION AND ANALYSIS

In this section, the computation time of the proposed SDFnT-based waveform design method is firstly analyzed. Then, in order to demonstrate the performance of the SDFnT-based angle estiamtioin method for non-stationary OFDM-LFM signals, comparisons between the proposed method and the FrFT-based target angle estimation method reported in the literature [39] in terms of performance of DoA estimation, and DoA-DoD estimation are presented. We consider a MIMO radar system with 2 transmitting arrays and 4 receiving arrays. The bandwidth of the OFDM-LFM waveform is 100 MHz and the duration is 2.56 us. The number of snapshot is 256 and the SNR is set to 10 dB. The simulation environment is based on MATLAB 2019a, on a computer with an Intel i5-10210U CPU Core.

A. COMPUTATION TIME OF WAVEFORM DESIGN

The time required to generate OFDM-LFM orthogonal waveforms using the SDFnT method and the FrFT method is shown in Table 1. N stands for the number of subcarriers in OFDM-LFM, and it ranges from 256 to 1792 in steps of 512. The time results are averaged after 500 Monte Carlo simulations. Table 1 shows that the computational time needed to produce orthogonal waveforms using the proposed SDFnT approach is shorter than that needed to produce them using the FrFT method for the same number of subcarriers, and that this time savings grows as the subcarrier count increases.

B. PERFORMANCE OF DoA ESTIMATION

In order to compare the computational times of FrFT method and proposed SDFnT method with single and multiple targets, figures 8 and 9 respectively show the computed timings for various numbers of snapshots K and time-frequency surface traversal times α. It is evident that the proposed SDFnT-based method requires less complicated processing and can cut the computational time by roughly 20%.

To analyze the accuracy of the proposed method with respect to angle with various signal qualities, the SNR is set to vary from -15 dB to 10 dB with an interval of 1 dB, and $\theta 1 = 15°$ and $\theta 2 = 20°$. After 500 Monte Carlo simulations, the RMSEs of the target parameters are shown as in Fig. 10. It can be seen that neither method can estimate

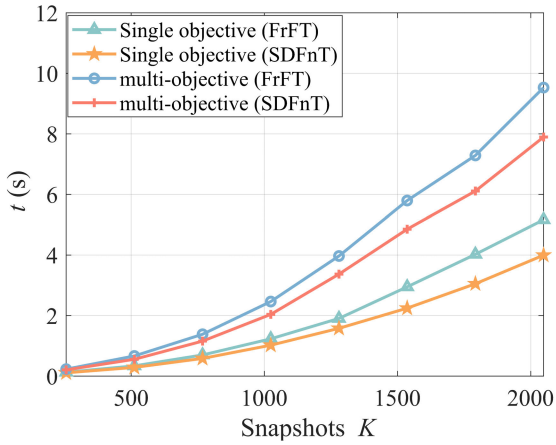

FIGURE 8. The computational time of SDFnT methods and FrFT method for traversing snapshot numbers.

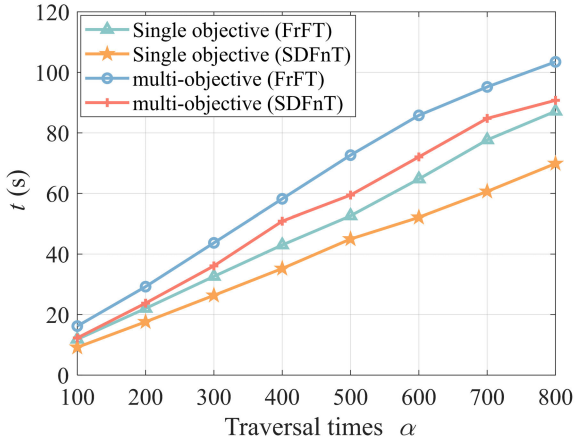

FIGURE 9. The computational time of SDFnT methods and FrFT method for traversing search times.

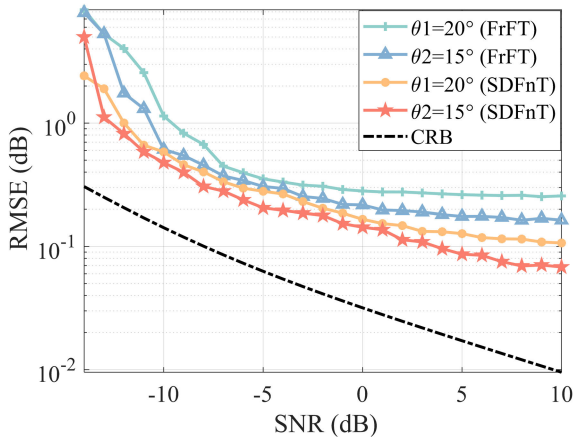

FIGURE 10. RMSE of SDFnT methods and FrFT method of Traversing SNR.

the target angles when the SNR is less than 10 dB. This is because, the peak value following signal transformation to the chirp domain is totally hidden by the noise signal. However, because the FrFT method computes the trigonometric function numerous times, which demands more accuracy, it has a little lower angle estimation accuracy than the novel SDFnT based method.

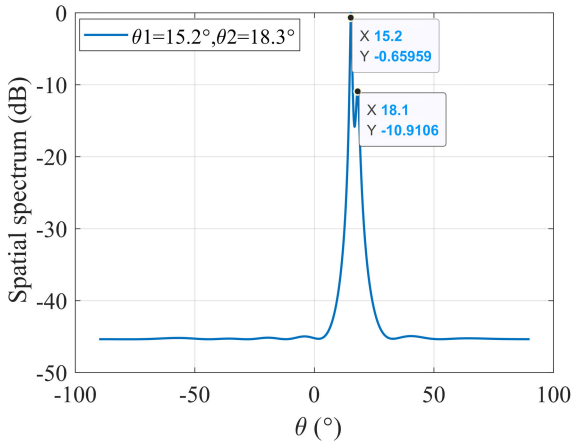

FIGURE 11. Multi-targets MUSIC spatial spectrum.

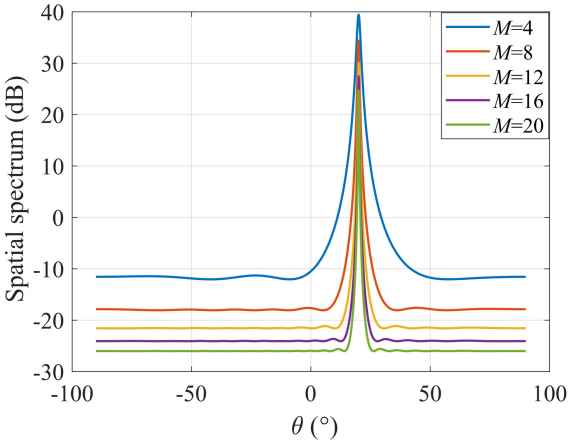

FIGURE 12. Single-objective SDFnT-MUSIC spatial spectrum traversing array elements.

Figure 11 shows the MUSIC spatial spectrum, where the angle θ is searched from $-90°$ to $-90°$ and $\Delta\theta = 0.01°$ represents the angular step value. The real incident angles for the two targets are $\theta 1 = 15.2°$ and $\theta 2 = 18.3°$. It is not difficult to find that the proposed SDFnT-based method has high angle estimate accuracy even when the two targets are quite near to one another.

Figures 12 and 13 depict how the number of array elements affects the precision of single- and multi-target angle estimates. The findings demonstrate that the accuracy of angle estimate is strongly influenced by the number of array elements, and that target angle estimation performance greatly improves with increasing array element number.

Figure 14 depicts how the estimating performance is affected by the number of snapshots. Naturally, increasing the number of snapshots can also increase the accuracy of the angle estimation, but by comparing the cases of the number of snapshots $K = 128$ and $K = 256$, we can see that the increase in snapshots does not significantly improve performance. However, we already know from Fig. 8 that the increase in snapshots increases the computation time significantly, so we need to choose the appropriate number of snapshots to get better performance and less computation time.

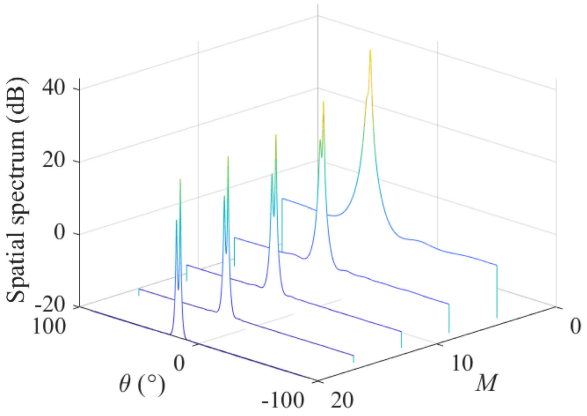

FIGURE 13. Mulit-objective SDFnT-MUSIC spatial spectrum traversing array elements.

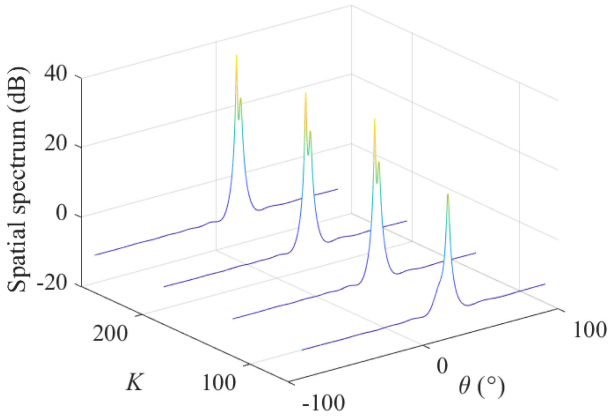

FIGURE 14. SDFnT-MUSIC spatial spectrum of ergodic snapshots.

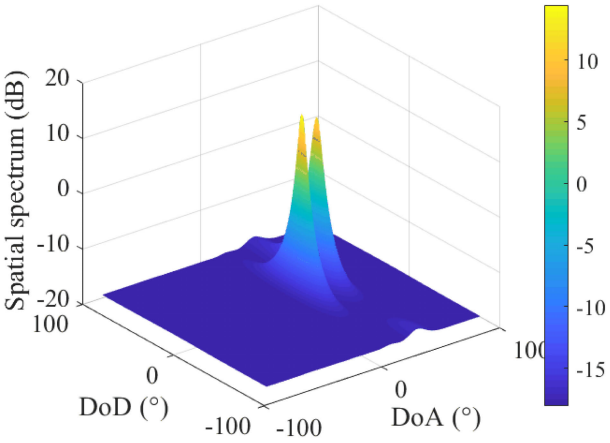

FIGURE 15. 2D-MUSIC algorithm based on SDFnT.

C. PERFORMANCE OF DoA-DoD ESTIMATION

The bistatic MIMO radar can detect the target even in the absence of additional information like target range according to the DoD and DoA information. This section uses the SDFnT method and the 2D-MUSIC algorithm to jointly estimate the transceiver angle for non-stationary signals.

Figures 15 and 16 display the results of the 2D-MUSIC angle estimation based on the SDFnT method and its top view, demonstrating how the method can jointly estimate

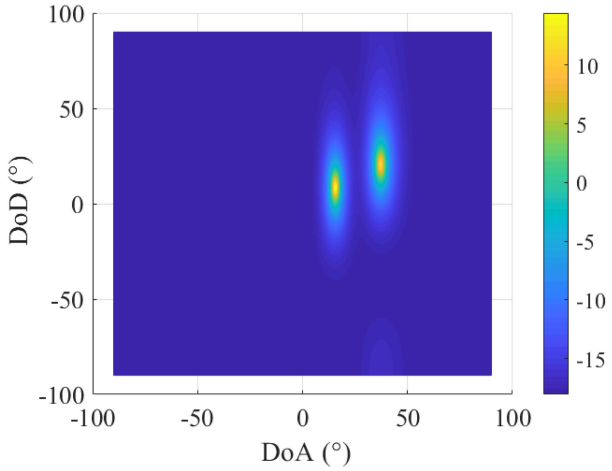

FIGURE 16. The overlooking function of 2D-MUSIC algorithm based on SDFnT.

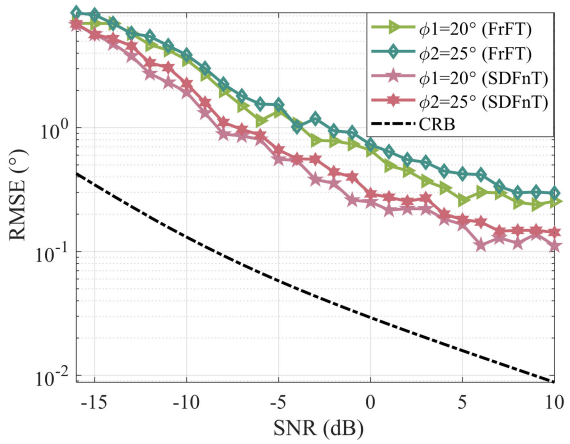

FIGURE 17. The RMSE of DoD when traversing SNR based on SDFnT-MUSIC method.

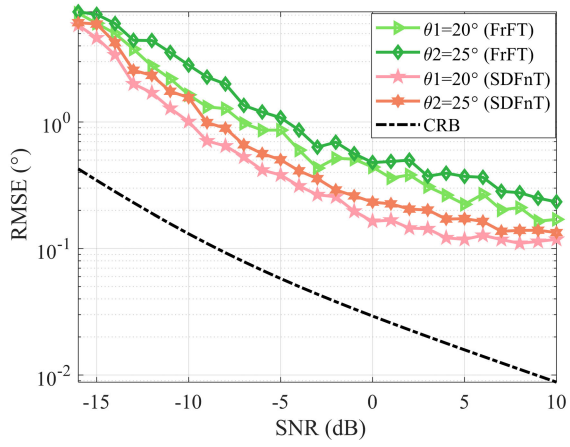

FIGURE 18. The RMSE of DoA when traversing SNR based on SDFnT-MUSIC method.

the transceiver angle of non-stationary signals while also estimating the target number when the number of sources is unknown. The RMSEs of the DoD and DoA estimates in terms of SNR are shown in Fig. 17 and Fig. 18, where $\phi 1$ and $\phi 2$ represent DoD, $\theta 1$ and $\theta 2$ represent DoA. As expected, the proposed SDFnT method consistently achieves high accuracy DoD and DoA estimations in the majority of the considered SNR region (SNR $>$ -10 dB) and the performance of angle estimation using the proposed approach in this paper is marginally superior to that using the FrFT method.

V. CONCLUSION

This paper first proposed an efficient OFDM-LFM waveform design method, which can efficiently generates orthogonal LFM signals with unlimited number of subcarrier, based on a novel scale discrete Fresnel transform with the kernel function as a set of orthogonal LFM with adjustable chirp rate. Then we further proposed a novel angle estimation method for OFDM-LFM-based MIMO systems by combining the SDFnT method with the high-resolution MUSIC algorithm. This approach turns the time-varying steering vector into a non-time-varying steering vector in the chirp domain, allowing the classic subspace algorithm to be used for high-resolution angle estimation. Simulation results show that the proposed methods have lower computational complexity and better estimate performance than the FrFT-based approaches. In addition, because of their compatibility with the FFT, the proposed SDFnT-based methods have the extra benefit of being simple to implement in the existing OFDM systems. Furthermore, since the SDFnT has an inverse transform, it can be utilized for modulation and demodulation in multicarrier communication systems, as well as the development of innovative joint radar and communication systems in future.

REFERENCES

[1] D. W. Bliss and K. W. Forsythe, "Multiple-input multiple-output (MIMO) radar and imaging: Degrees of freedom and resolution," in *Proc. 37th Asilomar Conf. Signals, Syst. Comput.*, Nov. 2003, pp. 54–59.
[2] J. Li and S. Petre, "MIMO radar signal processing," Tech. Rep., 2009, pp. 1–64.
[3] T. D. Backes, "Parameter identifiability in a phased-subarray MIMO radar," in *Proc. IEEE Aerosp. Conf.*, Mar. 2014, pp. 1–6.
[4] Y. Petillot, C. Du, and J. S. Thompson, "Predicted detection performance of MIMO radar," *IEEE Signal Process. Lett.*, vol. 15, pp. 83–86, 2008.
[5] K. W. Forsythe, D. W. Bliss, and G. S. Fawcett, "Multiple-input multiple-output (MIMO) radar: Performance issues," in *Proc. Conf. Rec. 38th Asilomar Conf. Signals, Syst. Comput.*, Nov. 2004, pp. 310–315.
[6] F. Meinl, M. Stolz, M. Kunert, and H. Blume, "An experimental high performance radar system for highly automated driving," in *IEEE MTT-S Int. Microw. Symp. Dig.*, Mar. 2017, pp. 71–74.
[7] J. Suh, J. Lee, G.-T. Gil, and S. Hong, "Time-and-frequency hybrid multiplexing for flexible ambiguity controls of DFT-coded MIMO OFDM radar," *IEEE Access*, vol. 9, pp. 137793–137808, 2021.
[8] N. Levenon, "Multi frequency complementary phase-coded radar signal," *ET Radar Sonar Navig.*, vol. 147, no. 6, pp. 272–284, Dec. 2000.
[9] B. J. Donnet and I. D. Longstaff, "Combining MIMO radar with OFDM communications," in *Proc. Eur. Radar Conf.*, Manchester, U.K., Sep. 2006, pp. 37–40.
[10] Y.-H. Cao, X.-G. Xia, and S.-H. Wang, "IRCI free colocated MIMO radar based on sufficient cyclic prefix OFDM waveforms," *IEEE Trans. Aerosp. Electron. Syst.*, vol. 51, no. 3, pp. 2107–2120, Jul. 2015.
[11] S. H. Wang, C. P. Li, K. C. Lee, and H. J. Su, "A novel low-complexity precoded OFDM system with reduced PAPR," *IEEE Trans. Signal Process.*, vol. 63, no. 6, pp. 1366–1376, Mar. 2015.
[12] F. A. P. de Figueiredo, N. F. T. Aniceto, J. Seki, I. Moerman, and G. Fraidenraich, "Comparing f-OFDM and OFDM performance for MIMO systems considering a 5G scenario," in *Proc. IEEE 2nd 5G World Forum (5GWF)*, Sep. 2019, pp. 532–535.

[13] J.-H. Kim, M. Younis, A. Moreira, and W. Wiesbeck, "A novel OFDM chirp waveform scheme for use of multiple transmitters in SAR," *IEEE Geosci. Remote Sens. Lett.*, vol. 10, no. 3, pp. 568–572, May 2013.
[14] J. H. Kim, M. Younis, A. Moreira, and W. Wiesbeck, "Spaceborne MIMO synthetic aperture radar for multimodal operation," *IEEE Trans. Geosci. Remote Sens.*, vol. 53, no. 5, pp. 2453–2466, May 2015.
[15] S.-J. Cheng, W.-Q. Wang, and H.-Z. Shao, "Spread spectrum-coded OFDM chirp waveform diversity design," *IEEE Sensors J.*, vol. 15, no. 10, pp. 5694–5700, Oct. 2015.
[16] W.-Q. Wang, "MIMO SAR OFDM chirp waveform diversity design with random matrix modulation," *IEEE Trans. Geosci. Remote Sens.*, vol. 53, no. 3, pp. 1615–1625, Mar. 2015.
[17] J. Shang, Z. Wang, L. Zhou, and L. Zhao, "A joint time-frequency synchronization algorithm for FrFT-OFDM systems and its hardware implementation," in *Proc. 15th IEEE Int. Conf. Commun. Technol.*, Nov. 2013, pp. 190–195.
[18] K. C. K. Chen, Y. L. Y. Liu, and W. Z. W. Zhang, "Study on integrated radar-communication signal of OFDM-LFM based on FRFT," in *Proc. IET Int. Radar Conf.*, 2015, pp. 1–6.
[19] A. R. Nafchi, F. Sanz Estevez, E. Hamke, and R. Jordan, "Applying the FRFT to an OFDM system for Li-Fi: A design experiment for peace engineering education," in *Proc. World Eng. Educ. Forum Global Eng. Deans Council (WEEF-GEDC)*, Nov. 2018, pp. 1–4.
[20] M. D. Larsen, A. L. Swindlehurst, and T. Svantesson, "Performance bounds for MIMO-OFDM channel estimation," *IEEE Trans. Signal Process.*, vol. 57, no. 5, pp. 1901–1916, May 2009.
[21] R. Shafin, L. Liu, J. Zhang, and Y.-C. Wu, "DoA estimation and capacity analysis for 3-D millimeter wave massive-MIMO/FD-MIMO OFDM systems," *IEEE Trans. Wireless Commun.*, vol. 15, no. 10, pp. 6963–6978, Oct. 2016.
[22] Y. C. Lin, T. S. Lee, Y. H. Pan, and K. H. Lin, "Low-complexity high-resolution parameter estimation for automotive MIMO radars," *IEEE Access*, vol. 8, pp. 16127–16138, 2020.
[23] D. Werbunat, B. Meinecke, B. Schweizer, J. Hasch, and C. Waldschmidt, "OFDM-based radar network providing phase coherent DOA estimation," *IEEE Trans. Microw. Theory Techn.*, vol. 69, no. 1, pp. 325–336, Jan. 2021.
[24] F. Zhang, G. Bi, and Y. Q. Chen, "Tomography time-frequency transform," *IEEE Trans. Signal Process.*, vol. 50, no. 6, pp. 1289–1297, Jun. 2002.
[25] P. Rao and F. J. Taylor, "Estimation of instantaneous frequency using the discrete Wigner distribution," *Electron. Lett.*, vol. 4, no. 26, pp. 246–248, 1990.
[26] R. N. Czerwinski and D. L. Jones, "Adaptive short-time Fourier analysis," *IEEE Signal Process. Lett.*, vol. 4, no. 2, pp. 42–45, Feb. 1997.
[27] Q. Lin, T. Ran, Z. Siyong, and W. Yue, "Adaptive time-varying filter for linear FM signal in fractional Fourier domain," in *Proc. 6th Int. Conf. Signal Process.*, Aug. 2002, pp. 1425–1428.
[28] A. B. Gershman and M. G. Amin, "Wideband direction-of-arrival estimation of multiple chirp signals using spatial time-frequency distributions," *IEEE Signal Process. Lett.*, vol. 7, no. 6, pp. 152–155, Jun. 2000.
[29] F. Chen, T. Zhou, W. Yi, L. Kong, and B. Zhai, "Passive direct position determination of multiple emitters transmitting unknown LFM signals," in *Proc. IEEE Radar Conf. (RadarConf)*, Apr. 2018, pp. 1129–1133.
[30] X. Wang, B. Li, H. Yang, and W. Lu, "Off-grid DOA estimation for wideband LFM signals in FRFT domain using the sensor arrays," *IEEE Access*, vol. 7, pp. 18500–18509, 2019.
[31] H. Guo, G. A. Sitton, and C. S. Burrus, "The quick discrete Fourier transform," in *Proc. IEEE Int. Conf. Acoust., Speech Signal Process.*, Apr. 1994, pp. III/445–III/448.
[32] T. Ran, P. Xianjun, S. Yu, and Z. Xinghao, "A novel discrete fractional Fourier transform," in *Proc. CIE Int. Conf. Radar*, Oct. 2001, pp. 1027–1030.
[33] X. Ouyang and J. Zhao, "Orthogonal chirp division multiplexing for coherent optical fiber communications," *J. Lightw. Technol.*, vol. 34, no. 18, pp. 4376–4386, Sep. 15, 2016.
[34] Y. Yu, W. Wang, X. Ouyang, Z. Wang, and J. Zhao, "Discrete Fresnel transform spread OFDM for coherent optical fiber communication," *IEEE Photon. Technol. Lett.*, vol. 30, no. 1, pp. 91–94, Jan. 1, 2018.
[35] L. G. D. Oliveira, M. B. Alabd, B. Nuss, and T. Zwick, "An OCDM radar-communication system," in *Proc. 14th Eur. Conf. Antennas Propag. (EuCAP)*, Mar. 2020, pp. 1–5.
[36] C. Fang, H. Zishu, L. Hongming, and L. Jun, "The parameter setting problem of signal OFDM-LFM for MIMO radar," in *Proc. Int. Conf. Commun., Circuits Syst.*, May 2008, pp. 876–880.
[37] R. O. Schmidt, "Multiple emitter location and signal parameter estimation," *IEEE Trans. Antennas Propag.*, vol. AP-34, no. 3, pp. 276–280, Mar. 1986.
[38] X. Zeng, Z. Li, H. Huang, and G. Sun, "Focused passive synthetic aperture," in *Proc. IEEE Youth Conf. Inf., Comput. Telecommun.*, Nov. 2010, pp. 158–161.
[39] C. Fang, H. Zishu, L. Hongming, and L. Jun, "The parameter setting problem of signal OFDM-LFM for MIMO radar," in *Proc. Int. Conf. Commun., Circuits Syst.*, May 2008, pp. 876–880.

JINGQI WANG (Member, IEEE) received the B.E. degree in communication engineering from the Nanjing University of Aeronautics and Astronautics, Nanjing, China, in 2003, and the M.E. and Ph.D. degrees in electromagnetic field and microwave technology from Southeast University, Nanjing, in 2006 and 2011, respectively.

She is currently a Lecturer with the School of Electronic and Optical Engineering, Nanjing University of Science and Technology, Nanjing. Her research interests include the signal processing for multicarrier radar, waveform design for joint radar and communication systems, and linearization technologies for power amplifier.

PINGPING WANG received the B.S. degree in electronic information engineering from the University of South China, Hunan, China, in 2020. She is currently pursuing the M.S. degree in electromagnetic field and microwave technology with the Nanjing University of Science and Technology, Nanjing, China. Her current research interests include radar signal processing and joint radar and communication.

FAN LUO received the B.S. degree in telecommunications engineering from the Zijin College, Nanjing University of Science and Technology, Nanjing, China, in 2019, where he is currently pursuing the M.S. degree in electronics and communications engineering. His research interests include joint radar and communication.

WEN WU (Senior Member, IEEE) received the Ph.D. degree in electromagnetic field and microwave technology from Southeast University, Nanjing, China, in 1997.

He is currently a Professor with the School of Electronic and Optical Engineering, Nanjing University of Science and Technology, where he is also the Associate Director of the Ministerial Key Laboratory of JGMT. He has authored or coauthored over 300 journals and conference papers and has submitted over 30 patent applications. His current research interests include micro-wave and millimeter-wave theories and technologies, microwave and millimeter-wave detection, and multimode compound detection. He was a recipient of six times of ministerial and provincial-level science and technology awards.